Mass Spectrometry

How to cite:
International Edition: doi.org/10.1002/anie.202216969
German Edition: doi.org/10.1002/ange.202216969

Immuno-Desorption Electrospray Ionization Mass Spectrometry Imaging Identifies Functional Macromolecules by Using Microdroplet-Cleavable Mass Tags

*Xiaowei Song, Qingce Zang, Chao Li, Tianhao Zhou, and Richard N. Zare**

Abstract: We present immunoassay-based desorption electrospray ionization mass spectrometry imaging (immuno-DESI-MSI) to visualize functional macromolecules such as drug targets and cascade signaling factors. A set of boronic acid mass tags (BMTs) were synthesized to label antibodies as MSI probes. The boronic ester bond is employed to cross-link the BMT with the galactosamine-modified antibody. The BMT can be released from its tethered antibody by ultrafast cleavage of the boronic ester bond caused by the acidic condition of sprayed DESI microdroplets containing water. The fluorescent moiety enables the BMT to work in both optical and MS imaging modes. The positively charged quaternary ammonium group enhances the ionization efficiency. The introduction of the boron element also makes mass tags readily identified because of its unique isotope pattern. Immuno-DESI-MSI provides an appealing strategy to spatially map macromolecules beyond what can be observed by conventional DESI-MSI, provided antibodies are available to the targeted molecules of interest.

Desorption electrospray ionization (DESI) is the most used method for ambient mass spectrometry imaging (MSI). It employs charged spraying microdroplets to softly ionize molecules from a biological tissue under open, atmospheric conditions.[1] A variety of chemical species were readily investigated by DESI-MSI such as small organic drugs, carbohydrates, amino acids, carboxylates, amines, ketones, aldehydes, nucleotides, lipids, peptides, etc.[2] Although these endogenous metabolites and lipids well describe the metabolism status and its alteration, it is also important to associate them with macromolecules for insight into the sophisticated molecular regulation behind disease progression or drug action. These macromolecules mainly include membrane protein receptors, carriers, enzymes, and signaling factors, which are not only functional molecules to implement the biological process but also potential diagnostic biomarkers or therapeutic targets.[3]

Nonetheless, the current DESI-detectable species are mainly small organic molecules with a molecular weight of less than 2000 Da. Direct protein analysis and imaging from tissue samples might present a special challenge for DESI-MS because of their ultrahigh molecular weight, poor ionization efficiency, and low abundance. Some efforts and breakthroughs have been made to achieve protein imaging by the addition of ammonium bicarbonate, spray desorption collection-based off-line analysis, native DESI, nano-DESI, or DESI in combination with FAIMS.[4] Nevertheless, a more versatile strategy is urgently needed to image any protein by the DESI-MSI technique without any limitation placed on its type and molecular weight.

The immunoassay-based imaging strategy provides a feasible way to visualize the distribution of specific macromolecules across a tissue. A labeled molecule cross-linked to the bio-specific antibody will report the position and amount of a target macromolecule. The optical signal-based image presentation, such as fluorescent tags in immunofluorescent microscopy (IFM), has limited channels for multiplex imaging from the bandwidth-caused signal overlay issue.[5] Because a mass analyzer enables processing thousands of available ion channels to present molecular phenotype information, the MS-based immunoassay also gains successful instrument development of mass cytometry.[6] The mass tag and cleavable chemical bond are critical designs for mass cytometry. Rare metal mass tags can be cleaved by a high-energy ion beam or laser photons in a MIBI-TOF,[7] or

[*] Dr. X. Song, Prof. R. N. Zare
Department of Chemistry, Stanford University
Stanford, CA-94305 (USA)
E-mail: rnz@stanford.edu

Dr. X. Song
Department of Chemistry, Fudan University
Shanghai, 200016 (China)

Dr. Q. Zang
Institution of Materia Medica, Chinese Academy of Medical Science and Peking Union Medical College
Beijing (China)

Dr. C. Li
Department of Medicine, Stanford University School of Medicine
Palo Alto, CA-94304 (USA)

Dr. T. Zhou
National Clinical Research Center of Cancer, Tianjin Medical University
Tianjin, 300060 (China)

SIMS system.[8] Organic molecule such as peptide, choline, or rhodamine derivatives can also serve as mass tags. They can be either online released through photocleavage of weak S–C(triphenylmethyl) bond,[9] electrochemical reduction of S–Au bond,[10] or offline released through acid-hydrolysis of ester bond.[11] Nonetheless, there is still no mass tags and cleavable chemical bond design reported for the purpose of DESI-MSI to visualize the spatial distribution of macromolecules.

Micron-sized water droplets generated by DESI under positive high voltage are rich in protons (H^+) around the air-solvent interface.[12] It is reported that the acid-catalyzed organic reaction in the microdroplet can be accelerated and completed at the 10^2 microseconds time scale.[13] In comparison, the impact between the DESI sprayed microdroplets and tissue sample is at the millisecond time scale. This interaction time is sufficient for the strong acidic microdroplet to hydrolyze the ester bond and release the mass tag from its tethered antibody. Boronic acid can reversibly bind with and release from the diol compound when the pH varies from basic to acidic conditions.[14] Given the special chemical properties of boronate ester and spraying water microdroplet's pH, we developed a series of water microdroplet-cleavable mass tags. This method is named as "immuno-DESI-MSI", which enables conventional DESI-MSI to map functional macromolecules across a tissue section.

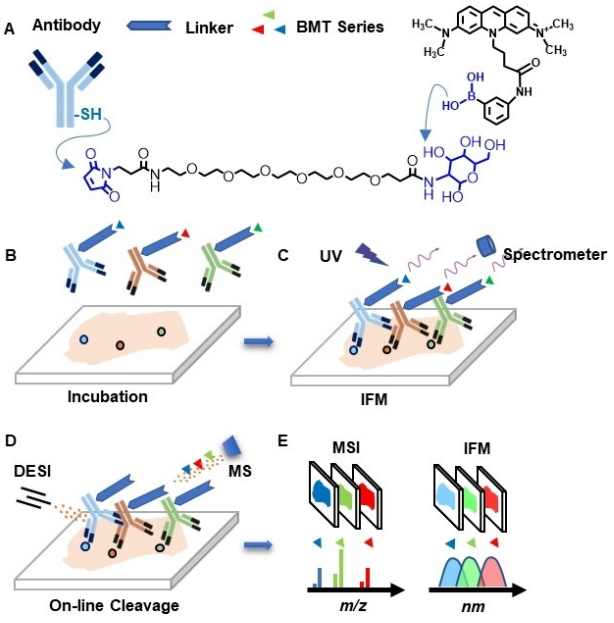

Scheme 1. The designed probe's structure and general workflow of the immuno-DESI-MSI. A) Key elements of the designed probe include antibody for biospecific recognition, cross-linker, and boronate mass tag (BMT). BMT495 is presented here as the example; B) A cryosection was incubated with multiplex BMT-labeled antibodies. C) Excessive BMT-labeled antibodies washup and immunofluorescence microscopy (IFM) imaging; D) Acidic water microdroplets were sprayed onto the incubated cryosection to cleave the BMTs from the antibodies and transported them into the mass spectrometer. E) BMT ion images can be constructed to visualize the corresponding macromolecules. Meanwhile, the fluorescent images can also be observed under a microscope.

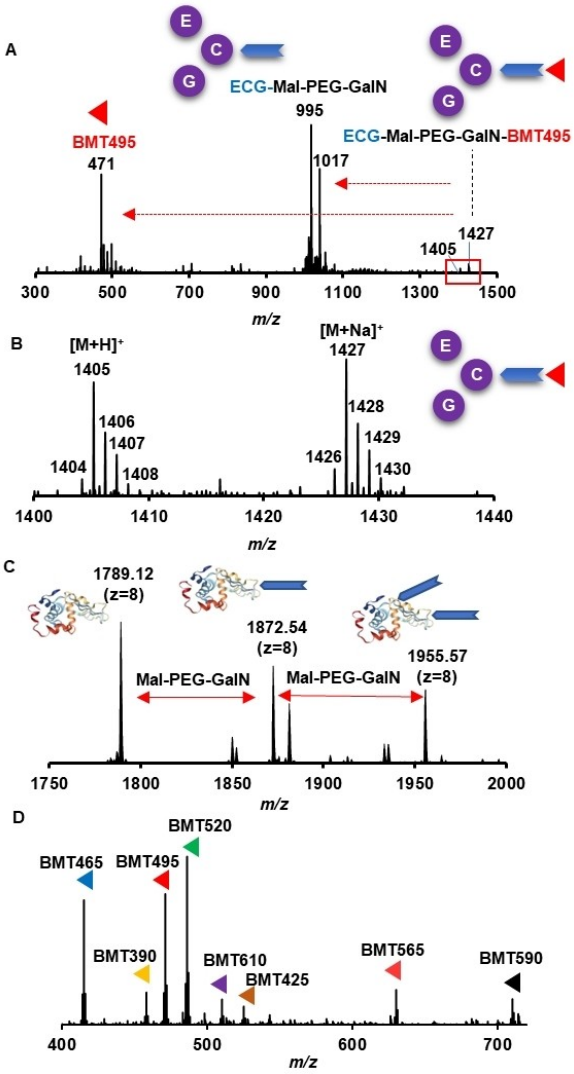

Figure 1. MS characterization of the BMT-labelled model peptide and its instant release. A) cross-linker-modified glutathione (ECG); B) final product of BMT495-modified ECG; C) Cross-linker modified lysozyme generated by the microdroplet spray-induced boronate ester bond cleavage; D) eight BMT molecules online cleaved from the cross-linker modified lysozyme during the electrospray ionization.

Scheme 1 shows the general immuno-DESI-MSI workflow. The first step is the design and synthesis of the probe. It is composed of boronic acid mass tag (BMT), antibody (Ab), and cross-linker. The BMT is synthesized by reacting the fluorescent compound ATTO series N-hydroxysuccinimide ester (ATTO 390, 425, 465, 495, 520, 565, 590, 610), with the 3-aminophenylboronic acid (APBA) (See Figure S1 in the Supporting Information). The synthesized BMT molecules have bifunctional designs for both DESI-MSI and IFM. Its fluorescent structure can be observed under IFM. DESI-MSI is typically limited to the spatial resolution around 50–200 μm whereas optical resolution can reach 1 μm or less. Consequently, the combination allows sub-

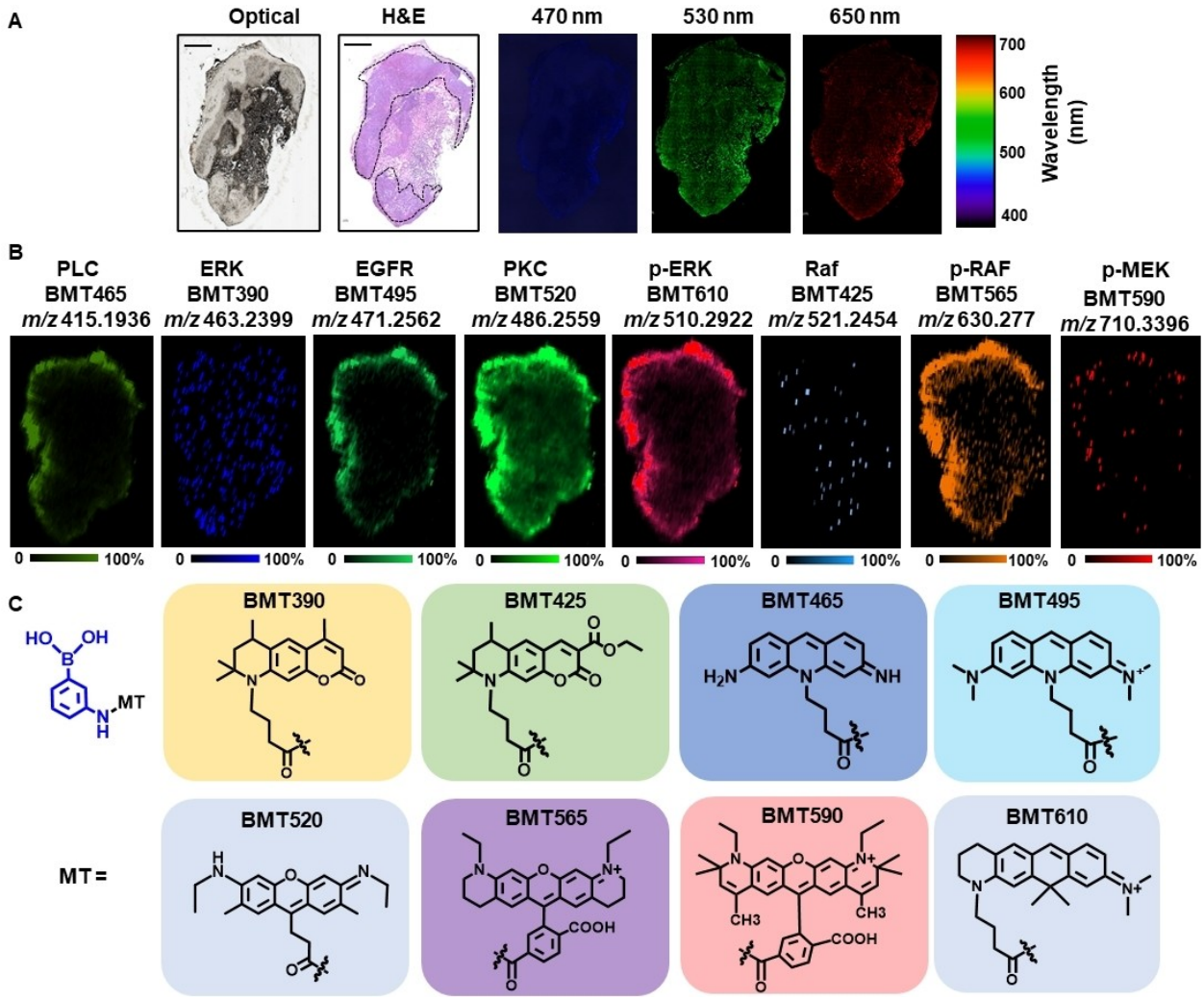

Figure 2. Cross-validation of images acquired by the IFM and immuno-DESI-MSI. A) Optical, H&E staining, and IFM images of xenograft tumor section, eight fluorescent tags were directly labelled on antibodies: The parenchyma region was delineated by the H&E staining; B) immuno-DESI-MS images of eight BMT-cross-linked antibodies. C) The chemical structures of the eight BMT molecules. Scale bars in the optical and H&E stain images represent 1.0 mm.

cellular resolution.[15] Meanwhile, the tertiary or quaternary amine group from the BMT has strong ionization efficiency for sensitive DESI-MSI detection. Additionally, the BMT ion can be easily differentiated from interfering peaks owing to its unique isotope distribution.

The antibody can specifically localize the targeted macromolecular antigen. The cross-linker (Mal-PEG-GalN) is synthesized from maleimide-PEG6-succinimidyl ester (Mal-PEG-SE) and galactosamine (GalN) by substituting the succinimidyl ester with the amine group from GalN. The double bond from the maleimide end of Mal–PEG–SE will add to the exposed thiol group on the antibody to complete the primary labeling (GalN–PEG–Mal–Ab). Thereafter, the BMT's boronic acid group can bind with the diol structure. (Scheme 1A).

The BMT synthesis is simple to carry out under mild conditions (Figure S1) and easily purified by chromatography using a small column (Table S1, and Figure S2–S4). The prepared BMT can be kept stable for at least one month under −20 °C storage condition. All steps of the Ab labeling, excessive cross-linker, and BMT removal can be complete within a 400 μL centrifugal filter unit (MW Cutoff: 3.0 kDa) to prevent severe loss of the small volume sample solution (Figure S5–S8). After probe preparation, the mixed BMT-Ab solution was incubated on the tissue cryosection. Each BMT-Ab will specifically recognize and bind with the corresponding macromolecular antigen (Scheme 1B). The excessive free BMT-Ab is washed away by an ammonium bicarbonate buffer solution (Scheme 1C). The boronate ester bond is then hydrolyzed by the acidic sprayed water microdroplets to release free BMT molecules for further desorption, ionization, and transport into the MS inlet for data acquisition (Scheme 1D). Thus, the DESI-MS image and IFM image can be sequentially collected for further analysis (Scheme 1E).

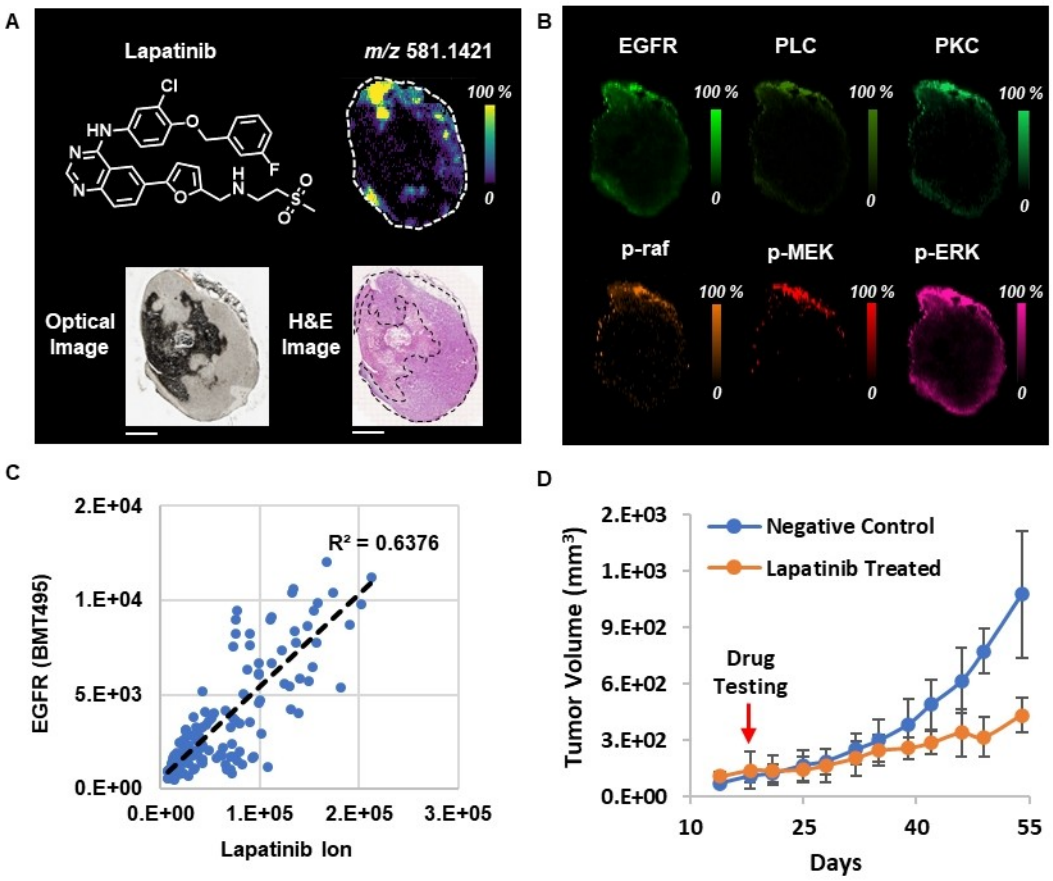

Figure 3. immune-DESI-MSI images of the six macromolecules in the EGFR pathways and its spatial correlation analysis with the anti-EGFR drug Lapatinib. A) The chemical structure of lapatinib, and its optical image, H&E staining image, as well as ion images; B) Immuno-DESI-MSI images of the six macromolecules in the EGFR pathways that have statistical significance compared to them in the model control group; Each color bar denotes the relative intensity ranging from 0 to 100%. C) Pixel-by pixel spatial correlation analysis between EGFR and lapatinib across the tumor parenchyma region; D) Pharmacological trial to verify the anti-tumor effect of lapatinib. Blue curve presents the growth of the tumor without drug treatment and red with the drug treatment, started at the 15th day. The error bars denote the standard deviations in each group of three measurements. Scale bars in the optical and H&E stain images represent 1.0 mm.

The acid-induced boronate ester bond cleavage was first investigated using an electrospray ionization mass spectrometer (ESI-MS), which is frequently employed to generate microdroplets for online reaction process monitoring.[16] Glutathione was first selected as the model peptide to investigate the online BMT release. The BMT495-modified glutathione (ECG) water solution (pH 7.2) was directly nebulized into charged microdroplets under a positive 2.0 kV voltage. The BMT495 (m/z 471) and GalN-PEG-Mal-ECG ion (m/z 995 $[M+Na]^+$, and m/z 1017 $[M-H+2Na]^+$) can be rapidly generated (Figure 1A), with only a weak amount of remaining intact BMT495-GalN-PEG-Mal-ECG observed (m/z 1405 $[M+H]^+$, and m/z 1427 $[M+Na]^+$, Figure 1B). The whole cleavage process was completed within only 200 µs, given the sprayer-to-inlet distance of 16 mm and the estimated linear velocity around 80 m s^{-1}.[17] In comparison, the normal boronate ester cleavage time takes at least 1–3 minutes to complete in an acidic bulk solution.[14b]

Rapid boronate bond cleavage was also verified on BMT-modified lysozyme. Once injected into the ESI-MS, the cleaved lysozyme with 1–2 modified GalN-PEG-Mal cross-linkers (Figure 1C), and a series of BMT label molecule ions were immediately observed in the mass spectrum (Figure 1D). Their intensities varied because of their differences in molar concentrations, degree of labeling (DOL), and native ionization efficiencies due to structural diversity. Therefore, building the quantitation curves is a necessary step for making a comparison among different samples in further studies. To further confirm if the positively charged water microdroplet indeed cleaves the boronate bond, ultraviolet-visible (UV/Vis) spectroscopy was used to detect the intact structure of BMT495-GalN-PEG-Mal-lysozyme under the same pH of the bulk water solution. In contrast, when the sprayed product of BMT495-GalN-PEG-Mal-lysozyme was collected and filtered with an ultracentrifugal column, the UV/Vis signal at the maximum absorbance wavelength of 510 nm was not detectable (Fig-

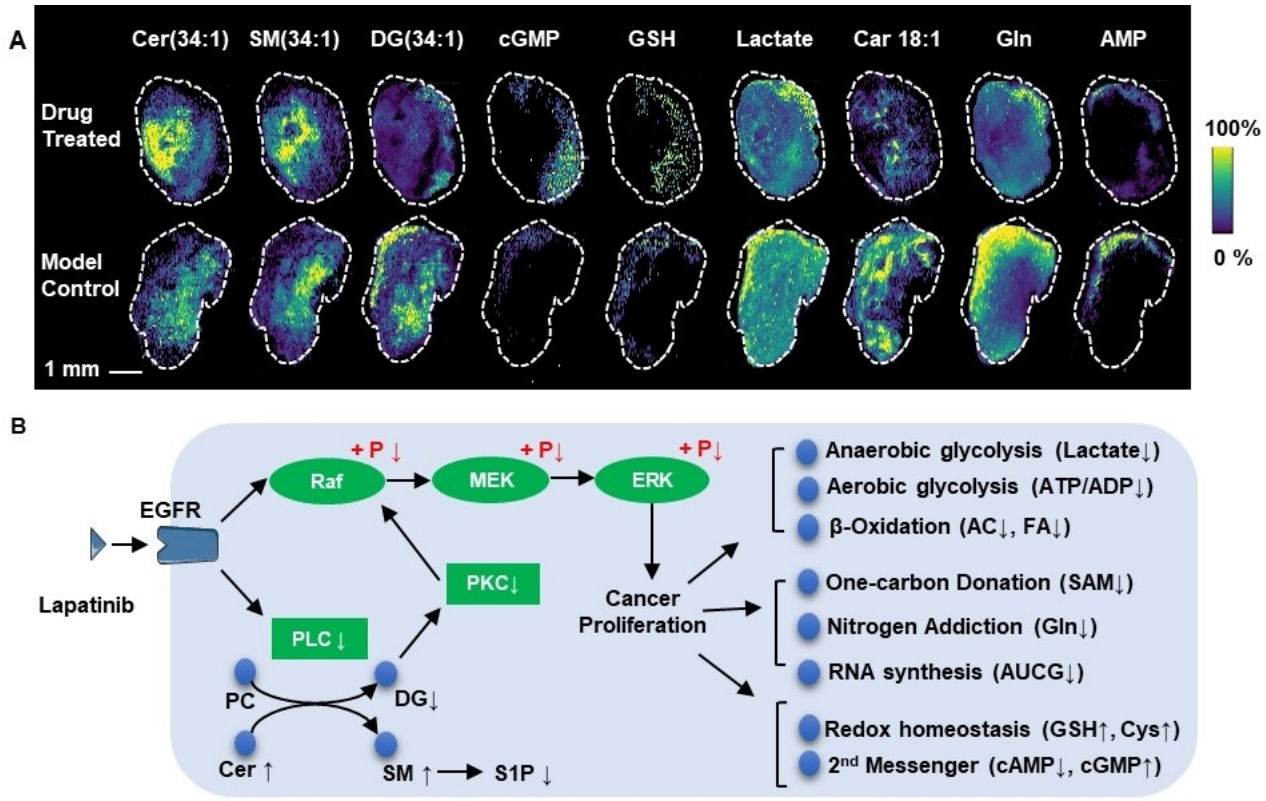

Figure 4. The molecular mechanism analysis integrated the drug, target, signaling pathway, and metabolomics acquired from the immuno-DESI-MSI. A) Representative metabolite markers associated with the Lapatinib action in the tumor parenchyma region; B) Diagram of the molecular mechanism for lapatinib anti-EGFR and its cascade signaling and downstream metabolism. Scale bars in the optical and H&E stain images represent 1.0 mm.

ure S9). This result again verifies the water microdroplet's critical role in the boronate ester bond cleavage.

The immunoglobulin G (IgG) was used as the model antibody for BMT labeling. UV/Vis spectroscopy successfully characterized the eight BMT-IgG products (Figure S10) under their featured maximum absorbance wavelengths (Table S2). The DOL values of the eight BMT molecules were also quantitatively estimated based on the Beer–Lambert Law. Their DOL values were averaged at 1.6 ± 0.1, meaning that each antibody molecule is bound with either 1 or 2 BMT labels. This result is consistent with the results previously achieved from the ESI-MS measurement for lysozyme. The online release and linear response of BMT ions were also investigated by DESI-MSI. A 1:1 (v/v) methanol-water solution was used as the spraying solvent under $+5.0$ kV operating voltage. A dilution series of BMT-modified IgG were deposited onto the polyvinylidene fluoride (PVDF) film. Because the positively charged IgG is strongly attached to the negatively charged PVDF surface, only the free BMT cleaved from IgG can be detected by DESI-MSI. All eight BMT ions were successfully released, and their ion intensities linearly increased with the amount of IgG, which ranged from 1 to 32 pmol mm^{-2} ($R^2 = 0.79$–0.98, Figure S11).

This result means that immuno-DESI-MSI also has the potential to quantitatively image those target macromolecules.

As a proof-of-concept, the clinical therapeutic target, the epithelial growth factor receptor (EGFR), as well as its cascade signaling factors (Raf, ERK, p-MEK, p-Raf, p-ERK), and associated two enzymes (PLC, PKC) were selected as target macromolecules.[18] Two sets of labeled antibodies specific to those EGFR pathway macromolecules were parallelly prepared and incubated on the tumor section. One set is directly labeled by eight ATTO NHS esters for the IFM test as a positive reference. Another set is cross-linked with the BMT labels for the immuno-DESI-MSI test (Table S2). The two imaging test results can be cross-validated with each other by spatial co-registration based on the previous report. As shown in Figure 2, the images achieved from the IFM were consistent with those from the immuno-DESI-MSI, proving the correctness of the MSI result. However, immuno-DESI-MS can separate the distribution of eight macromolecules indicated by the eight BMT labels which cannot be differentiated from the IFM images at the blue (470 nm), green (530 nm), and red (620 nm) fluorescence emission channels.

Additionally, eight macromolecules were mainly distributed in the parenchyma and shared a similar distribution pattern across the tumor section. This is because the

parenchyma is the tumor microcompartment that has high vascularization and contains most of the active cancer cells. The EGFR and its pathway in this region are highly expressed to facilitate uncontrolled proliferation and tumor growth.[19] The anti-tumor drug lapatinib (Figure 3A) was employed as a model compound. Similar distribution patterns of the eight EGFR pathway molecules were also observed from the lapatinib-treated tumor section (Figure 3B). Immuno-DESI-MSI quantitatively discovered that eight EGFR signaling molecules' expression levels in the lapatinib-treated groups were significantly down-regulated compared to those in the model group (Figure S12). The conventional DESI-MSI test visualized the distribution pattern of lapatinib ion (m/z 581.1421, $[M+H]^+$) close to the EGFR. The spatial co-localization analysis confirmed a highly positive correlation between lapatinib and its target EGFR, meaning that lapatinib can reach the tumor microcompartment enriched in EGFR (Figure 3C). These results are confirmed by the pharmacological test showing the significant inhibition in the tumor size and its growth rate by lapatinib intervention (Figure 3D).

After immuno-DESI-MSI helped to locate the lapatinib-actioned region, the downstream metabolic changes were further investigated through untargeted spatial metabolomics analysis across the region in which EGFR and lapatinib coexisted. There were 65 metabolites involved in 16 pathways severely influenced by the lapatinib's inhibition in the EGFR signaling (Table S3). One of the most typical examples is the phosphatidylcholine (PC)/diacyl glyceride (DG) conversion and ceramide (Cer)/sphingomyelin (SM) conversion, which are coupled with each other and catalyzed by the enzyme phospholipase C (PLC). The previous immuno-DESI-MSI result revealed that the PLC was down-expressed after the lapatinib intervention compared to the negative control group (Figure S12). As was shown in the Figure 4A, the PLC substrate Cer(34:1) was up-regulated whereas its two products PC(34:1), and DG(34:1) were down-regulated caused by PLC suppression. As secondary messenger molecules, the reduced DG then weakens the cascade activation of PKC, and phosphorylation of Raf, MEK, and ERK factors and their process of promoting cancer cell proliferation.

Apart from signaling regulation, lapatinib was also found to inhibit EGFR-mediated tumor growth through several other metabolism pathways (Figure 4B): (1) suppression of energy fueling from the Warburg effect (lactate), aerobic glycolysis (ATP, ADP), beta-oxidation (acylcarnitine (AC), and fatty acids (FA)); (2) blockage of the one-carbon unit donor from S-adenosyl methionine (SAM) and nitrogen source supply from glutamine addiction; (3) reduction of RNA synthesis substrates production (AMP, UMP, CMP, GMP, IMP); and (4) recovery of the redox homeostasis species such as glutathione, and cysteine (Table S4).

In summary, the acidic water microdroplets sprayed in DESI can rapidly cleave the boronate ester bond and release the BMT from the antibody. The immuno-DESI-MSI method has been successfully developed to visualize the spatial distribution of functional macromolecules associated with the drug target and its cascade signaling pathway. It enables visualizing macromolecules across a tissue with a resolution higher than conventional DESI-MSI by its fluorescent imaging function. Therefore, the upstream sophisticated pathway regulation acquired by immuno-DESI-MSI, and downstream metabolism information acquired from DESI-MSI can be well integrated for spatial multi-omics studies, which have great potential for the biomarker-based disease diagnosis and molecular mechanism investigation.

Acknowledgements

This work was supported by the Air Force Office of Scientific Research through the Multidisciplinary University Research Initiative (MURI) program (AFOSR FA9550-21-1-0170) and National Natural Science Foundation of China (ID. 81903575).

Conflict of Interest

The authors declare no conflict of interest.

Data Availability Statement

The data that support the findings of this study are available from the corresponding author upon reasonable request.

Keywords: Desorption Electrospray Ionization · Immunoassay · Mass Spectrometry Imaging · Mass Tag · Microdroplets

[1] R. G. Cooks, Z. Ouyang, Z. Takats, J. M. Wiseman, *Science* **2006**, *311*, 1566–1570.
[2] J. He, C. Sun, T. Li, Z. Luo, L. Huang, X. Song, X. Li, Z. Abliz, *Adv. Sci.* **2018**, *5*, 1800250.
[3] a) D. R. Ifa, L. S. Eberlin, *Clin. Chem.* **2016**, *62*, 111–123; b) T. Soudah, A. Zoabi, K. Margulis, *Mass Spectrom. Rev.* **2021**, *40*, 1–28. DOI: org/10.1002/mas.21736
[4] a) K. A. Douglass, A. R. Venter, *J. Mass Spectrom.* **2013**, *48*, 553–560; b) E. Honarvar, A. R. Venter, *J. Am. Soc. Mass Spectrom.* **2017**, *28*, 1109–1117; c) S. Ambrose, N. G. Housden, K. Gupta, J. Fan, P. White, H. Y. Yen, J. Marcoux, C. Kleanthous, J. T. S. Hopper, C. V. Robinson, *Angew. Chem. Int. Ed.* **2017**, *56*, 14463–14468; *Angew. Chem.* **2017**, *129*, 14655–14660; d) E. K. Sisley, O. J. Hale, I. B. Styles, H. J. Cooper, *J. Am. Chem. Soc.* **2022**, *144*, 2120–2128.
[5] R. M. Levenson, A. D. Borowsky, M. Angelo, *Lab. Invest.* **2015**, *95*, 397–405.
[6] a) C. Giesen, H. A. Wang, D. Schapiro, N. Zivanovic, A. Jacobs, B. Hattendorf, P. J. Schuffler, D. Grolimund, J. M. Buhmann, S. Brandt, Z. Varga, P. J. Wild, D. Gunther, B. Bodenmiller, *Nat. Methods* **2014**, *11*, 417–422; b) L. Kuett, R. Catena, A. Özcan, A. Plüss, Cancer Grand Challenges I-MAXT Consortium, P. Schraml, H. Moch, N. de Souza, B. Bodenmiller, *Nat. Cancer* **2022**, *3*, 122–133; c) M. Angelo, S. C. Bendall, R. Finck, M. B. Hale, C. Hitzman, A. D. Borowsky, R. M. Levenson, J. B. Lowe, S. D. Liu, S. Zhao, Y. Natkunam, G. P. Nolan, *Nat. Med.* **2014**, *20*, 436–442.

[7] M. B. Leeat Keren, S. Thompson, T. Risom, K. Vijayaragavan, D. M. Erin McCaffrey, R. Angoshtari, N. F. Greenwald, H. Fienberg, N. K. J. Wang, D. Kirkwood, G. Nolan, T. J. Montine, R. W. S. J. Galli, S. C. Bendall, M. Angelo, *Sci. Adv.* **2019**, *5*, eaax5851.
[8] H. Tian, L. J. Sparvero, T. S. Anthonymuthu, W. Y. Sun, A. A. Amoscato, R. R. He, H. Bayir, V. E. Kagan, N. Winograd, *Anal. Chem.* **2021**, *93*, 8143–8151.
[9] J. Yang, P. Chaurand, J. L. Norris, N. A. Porter, R. M. Caprioli, *Anal. Chem.* **2012**, *84*, 3689–3695.
[10] S. Xu, W. Ma, Y. Bai, H. Liu, *J. Am. Chem. Soc.* **2019**, *141*, 72–75.
[11] S. Chen, Q. Wan, A. K. Badu-Tawiah, *J. Am. Chem. Soc.* **2016**, *138*, 6356–6359.
[12] E. M. M. Girod, D. I. Campbell, R. G. Cooks, *Chem. Sci.* **2011**, *2*, 501–510.
[13] a) S. Banerjee, R. N. Zare, *Angew. Chem. Int. Ed.* **2015**, *54*, 14795–14799; *Angew. Chem.* **2015**, *127*, 15008–15012; b) J. K. Lee, H. G. Nam, R. N. Zare, *Q. Rev. Biophys.* **2017**, *50*, e2.
[14] a) R. Nishiyabu, Y. Kubo, T. D. James, J. S. Fossey, *Chem. Commun.* **2011**, *47*, 1106–1123; b) X. Wang, P. Bai, Z. Li, Q. F. Zhu, Z. Wei, Y. Q. Feng, *Angew. Chem. Int. Ed.* **2022**, *61*, e202208138; *Angew. Chem.* **2022**, *134*, e202208138.
[15] X. Yan, X. Zhao, Z. Zhou, A. McKay, A. Brunet, R. N. Zare, *Anal. Chem.* **2020**, *92*, 13281–13289.
[16] A. J. Ingram, C. L. Boeser, R. N. Zare, *Chem. Sci.* **2016**, *7*, 39–55.
[17] J. K. Lee, S. Kim, H. G. Nam, R. N. Zare, *Proc. Natl. Acad. Sci. USA* **2015**, *112*, 3898–3903.
[18] G. Lurje, H. J. Lenz, *Oncology* **2009**, *77*, 400–410.
[19] a) H. Lanaya, A. Natarajan, K. Komposch, L. Li, N. Amberg, L. Chen, S. K. Wculek, M. Hammer, R. Zenz, M. Peck-Radosavljevic, W. Sieghart, M. Trauner, H. Wang, M. Sibilia, *Nat. Cell Biol.* **2014**, *16*, 972–977; b) A. De Luca, A. Carotenuto, A. Rachiglio, M. Gallo, M. R. Maiello, D. Aldinucci, A. Pinto, N. Normanno, *J. Cell. Physiol.* **2008**, *214*, 559–567.

Manuscript received: November 17, 2022
Accepted manuscript online: January 9, 2023
Version of record online: ■■, ■■

Communications

Mass Spectrometry

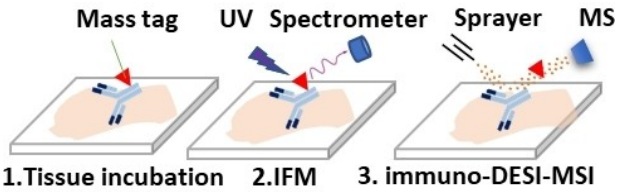

Water-microdroplet-cleavable, bifunctional boronate mass tags are introduced to conduct cell-resolved immunofluorescence imaging followed by multiplex immuno-desorption electrospray ionization mass spectrometry imaging.